Langmuir

Article

pubs.acs.org/Langmuir

Relationship Between Molecular Contact Thermodynamics and Surface Contact Mechanics

Nikolaos Nikogeorgos, Christopher A. Hunter, and Graham J. Leggett*

Department of Chemistry, University of Sheffield, Brook Hill, Sheffield S3 7HF, United Kingdom

Supporting Information

ABSTRACT: Measurements have been made of the adhesion and friction forces between organic monolayers in heptane/acetone mixtures using an atomic force microscope (AFM). It has been found that the contact mechanics are best modeled by treating the friction force as the sum of a load-dependent term (attributed to "molecular plowing") and an area-dependent term attributed to shearing (adhesion). The relative contributions of plowing and shearing are determined by the coefficient of friction, μ, and the surface shear strength τ. The transition from adhesion- to load-determined friction is controlled by the solvation state of the surface: solvated surfaces represent a limiting case in which the shear term approaches zero, and the friction-load relationship is linear, while in other circumstances, the friction-load relationship is nonlinear and consistent with Derjaguin–Muller–Toporov mechanics. A striking correlation has been observed between the concentration-dependence of the association constant (K_a) for the formation of 1:1 hydrogen-bonded complexes and the pull-off force F_a and surface shear strength τ for the same molecules when one partner is immobilized by attachment to an AFM probe and the other is adsorbed to a surface. Analysis of the concentration-dependence of F_a and τ enables the prediction of K_S with remarkably high precision, indicating that for these hydrogen bonding systems, the tip–sample adhesion is dominated by the H-bond thermodynamics. For mixed monolayers, H-bond thermodynamics dominate the interaction even at very low concentrations of the H-bond acceptor. Even for weakly adhering systems, a nonlinear friction-load relationship results. The variation in τ with the film composition is correlated very closely with the variation in F_a. However, the coefficient of friction varies little with the film composition and is invariant with the strength of tip–sample adhesion, being dominated by molecular plowing and, for sufficiently large concentrations of hydroxyl terminated adsorbates, the disruption of intramonolayer hydrogen bonding interactions.

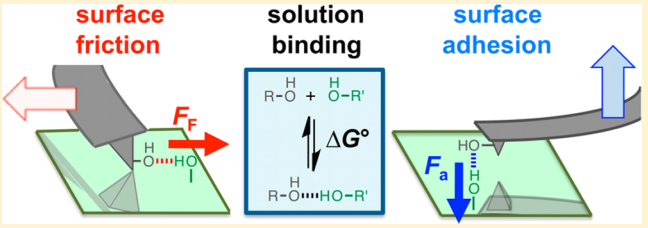

INTRODUCTION

In friction force microscopy (FFM),[1−3] measurements of the lateral deflection of an atomic force microscope (AFM) cantilever yield quantitative information on nanoscale friction, surface composition[4,5] and molecular organization.[6,7] Such measurements have promised to illuminate our understanding of not only tribological phenomena, but also the nature of intermolecular interactions at interfaces. However, fundamental questions remain unanswered. In particular, a unified model for the mechanics of the tip–sample interaction remains elusive: remarkably, many authors have modeled FFM using Amontons' law (in which the friction force is proportional to the load),[8] despite its being based on a macroscopic, multiasperity model for sliding contacts; while others have used single asperity mechanics approaches such as the Johnson–Kendall–Roberts (JKR)[9] and Derjaguin–Muller–Toporov (DMT)[10,11] models (in which there is a sublinear relationship between the friction force and the load). Without a clear understanding of the mechanics of the tip–sample contact, the use of FFM to study interfacial phenomena is, at best, qualitative. Moreover, while the role of surface adhesion is dominant in nanoscale molecular contacts, there is currently no clear understanding of the correlation between molecular interactions in single asperity contacts and in the bulk-phase. For chemists, the promise of access to quantitative data on intermolecular interactions has been an important motivation for exploring scanning probe techniques, so the absence of a unifying interpretational framework for SPM tribological data is a significant obstacle to their exploitation.

Although FFM measurements have been made in a variety of media, including air and liquids,[12,13] little consideration has been given, in general, to the role of the medium in determining the mechanics of the nanometer scale contact. However, it is now becoming clear that the probe environment has a profound effect on the contact mechanics, influencing not only the size of the friction force,[14] but also the nature of its dependence on the load.[15,16] Currently, there is no integrated framework for understanding the origin of these effects; there are thus substantial gaps in our understanding of how the medium influences measurements made by FFM. Often it is assumed that the dielectric properties of the medium modulate the adhesive interaction, but recent data have shown that this picture is unrealistic where polar interfaces are concerned. In a

Received: October 26, 2012
Published: December 3, 2012

   dx.doi.org/10.1021/la304246e | Langmuir 2012, 28, 17709−17717

recent study, we reported that for carboxylic acid terminated surfaces, many liquids with similar dielectric constants yield very different pull-off forces, and many liquids with very different dielectric constants yield similar pull-off forces.[17]

Previous work on FFM has, with few exceptions, used a single medium or a small number of media, making it difficult to draw reliable correlations between interfacial behavior and liquid properties. In recent work in the authors' laboratory, adhesion forces were measured between carboxylic acid functionalized SAMs in liquid mixtures containing a hydrocarbon (heptane) and a hydrogen bond acceptor (acetone or ethyl acetate).[17] It was found that the variation in the adhesion force F_a as a function of the composition of the liquid medium correlated closely with the variation in the free energy of interaction between carboxylic acids, and yielded a value for K_S, the association constant between the carboxylic acid group and the hydrogen bond acceptor in the liquid medium, that was in very close agreement with calculated values (confirmed in the bulk phase by spectroscopic measurements). It was found that a linear friction-load relationship was observed under conditions where there was extensive (almost complete) solvation of the SAM surface by the solution-phase hydrogen-bond acceptor, while DMT mechanics were observed in other circumstances. These findings were rationalized by postulating that the friction force could be treated, as others have suggested,[2,18] as the sum of a load-dependent term and a surface shear term:[17,19]

$$F_F = \mu(F_N + F_a) + \left(\frac{\tau}{K^{2/3}}\right)\pi R(F_N + F_a)^{2/3} \quad (1)$$

where τ is the surface shear strength, the stress needed to initiate or maintain sliding, determined by the interaction forces between the contacting surfaces,[3] K is the modulus and R is the radius of the probe. While fitting of this relationship yields $\tau/K^{2/3}$, the relationship between τ and the free energy has not been explored explicitly. Moreover, a significant limitation of our previous studies is that they addressed only the interactions between self-assembled monolayers (SAMs) of carboxylic acid terminated alkylthiolates.

In the present study, we report measurements on SAMs of hydroxyl terminated thiolates, and demonstrate an explicit correlation between the surface shear strength and the free energy of interaction at the hydroxylated surface. We also examine the relationship between contact mechanics and thermodynamics for mixed surfaces. We believe that these observations, while restricted to low-load conditions under which plastic deformation does not occur, provide a firm indication as to how the relationship between surface chemistry and the mechanics of molecular contacts may be understood in FFM.

EXPERIMENTAL SECTION

SAMs of HUT, 11-hydroxyundecyl-1-thiol (HUT, Sigma-Aldrich) were prepared by immersion of freshly deposited gold-coated (30 nm), chromium-primed (10 nm) glass slides in a 1 mM solution of the adsorbate in ethanol overnight. The slides (Menzel-Gläser 22 × 64 mm, no. 1.5) were cleaned for 45 min in "piranha" solution, a mixture of 30% H_2O_2 and 98% concentration sulfuric acid in the ratio 3:7 (caution: piranha solution is a strong oxidizing agent that has been known to detonate spontaneously upon contact with organic material, and should be handled with extreme care). Films of diethoxyphosphatoethyl-triethoxysilane (DPTS, Acros Organics) were prepared by immersing glass slides in a 1 mM solution of the adsorbate in dry toluene, under nitrogen in a Schlenk line, for 48 h. Substrates were prepared by cleaning in an RCA (Radio Cooperative America) cleaning solution (a mixture consisting of ammonium hydroxide (Analar), hydrogen peroxide and deionized water (Elga Pure Nanopore, 18.2 MΩ) in the ratio of 1:1:5 at 80 °C) for 40 min. Subsequently, samples were rinsed in fresh toluene and annealed in a vacuum oven (150 °C) for 1 h. Solvents (HPLC grade) were obtained from Fisher Scientific and used as received.

AFM measurements were made using a Digital Instruments Nanoscope IV Multimode instrument (Veeco Instruments, Santa Barbara, CA), using V-shaped silicon nitride probes (model NP, Veeco Instruments, Santa Barbara, CA) with a nominal normal force constant of 0.06 N m^{-1}. Measurements in liquids were made using a liquid cell fitted with either a silicone or Viton based elastomeric O-ring (Veeco Instruments, Santa Barbara, CA) depending on their compatibility with the liquid used in each experiment. The normal spring constant of the cantilever was obtained from the power spectral density of its thermal fluctuations in the resonant frequency domain, at room temperature, according to the method of Hutter and Bechhoefer.[20] The normal photodetector sensitivity was acquired from the slope of the linear part of a force curve at the repulsive regime, obtained on the flat regions of a silicon calibration grating (TGF11, Mikromash, Eesti, Tallinn, Estonia). Lateral forces were calibrated using the "wedge" method, introduced by Olgetree et al.[21] and developed by Varenberg et al.[22] using a commercially available silicon grating (the TGF11, Mikromash, Eesti, Tallinn, Estonia. The tip radius of curvature was determined by imaging a calibration grating (TGG01, Mikromash, Eesti, Tallinn, Estonia) at 0° and 90° scanning angles. The geometric mean radius of the tip was calculated by fit of a circle at the top of each image's profile and application of the Zenhausern model of deconvolution.[23]

Force curves were obtained at 200 locations on each sample, while two samples of each monolayer (MUT, DPTS) were examined with two different cantilevers in each environment. Pull-off forces were extracted from the unloading force curves using Carpick's Toolbox.[24] For friction measurements the instrument was operated with the long cantilever axis perpendicular to the fast scanning direction (2 Hz scanning speed), over areas of 1 × 1 μm^2. Friction forces were determined from trace-retrace loops acquired along single lines.

RESULTS AND DISCUSSION

Methodology. The present study addresses the interaction between an AFM tip and a surface functionalized with the molecular components of a hydrogen bond-forming pair. One of these functions as a hydrogen bond (H-bond) donor (D) and the other as an H-bond acceptor (A). Two systems have been compared, one symmetrical, in which the donor and acceptor are both hydroxyl groups; and the other asymmetric, in which a hydroxyl group is the donor and a phosphonate diester is the acceptor.

Consider first the behavior of D and A when free in solution. They may associate to form a 1:1 complex,

$$D + A \rightleftharpoons D \bullet A \quad (2)$$

with an equilibrium constant K_a. In a hydrocarbon solvent S1 (heptane in the present study), the solvent molecules may solvate the H-bond donor, albeit with low affinity:

$$D \bullet S1 + A \rightleftharpoons D \bullet A + S1 \quad (3)$$

The equilibrium constant associated with this interaction is K_1. If we introduce a second component S2 into the liquid medium, where S2 is a hydrogen bond acceptor (acetone in the present study), then this may compete with S1 to solvate the H-bond donor:

$$D \bullet S1 + S2 \rightleftharpoons D \bullet S2 + S1 \quad (4)$$

yielding an equilibrium constant K_S. The competition between S1, S2, and A for binding sites on the surface of the H-bond donor leads to a complex equilibrium:[25] S1 interacts only

dx.doi.org/10.1021/la304246e | Langmuir 2012, 28, 17709−17717

weakly with A to bind to D because it is nonpolar, but S2 competes more effectively because it is, itself, an H-bond acceptor. The value of K_a, the equilibrium constant for the formation of the hydrogen-bonded complex between D and A, will be different in a liquid mixture containing S2 than is the case in a mixture of D and A alone, because of the competition between S2 and A to bind to D. The value of K_a will vary with the solvation state of the H-bond donor (i.e., the extent to which D is solvated by S2).

In the same way, we hypothesize that the solvation state of an AFM probe functionalized with D will vary with the composition of the medium in which the measurement is made. When the H-bond donor molecules on the probe are extensively solvated, we predict that the interaction free energy will be reduced, leading to a decrease in the pull-off force and in the adhesive contribution to energy dissipation during sliding.

The thermodynamics of interaction between the H-bond donor and polar solvent molecules can be analyzed at a quantitative level. The equilibrium constant K_a for the formation of a 1:1 association complex between an H-bond donor D and an H-bond acceptor A varies with the composition of the solvent as shown in Figure 1(a). In a

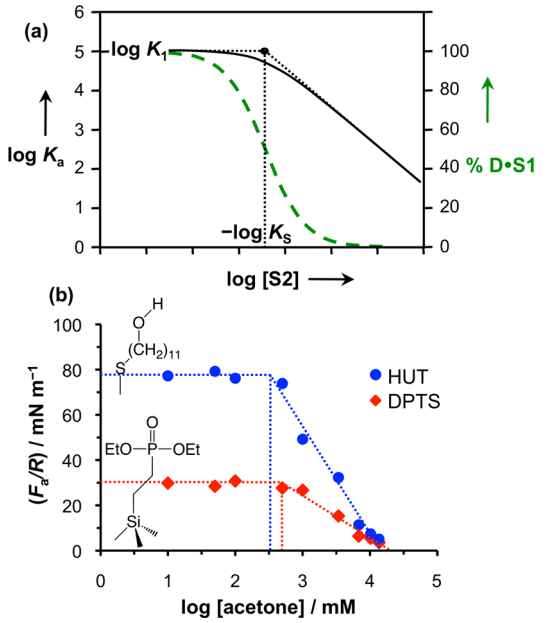

Figure 1. (a) Black line: variation in log K_a for the formation of a 1:1 complex between two solutes, D (an H-bond donor) and A (an H-bond acceptor) in mixtures of a nonpolar solvent (S1, heptane in the present study) and a polar solvent (S2, acetone in the present study) that is a strong H-bond acceptor but a weak H-bond donor. Green, dashed line: variation in solvation state of D (% D•S1). [Reproduced from Busuttil et al.[17]]. (b) Variation in the pull-off force F_a measured in heptane/acetone mixtures between AFM probes functionalized with a self-assembled monolayer of hydroxyl terminated thiols and films of either 11-hydroxyundecyl-1-thiol (HUT) or diethoxy-phosphatoethyl-triethoxysilane (DPTS). The adhesion force has been scaled to the probe radius (small variations were measured) and plotted as F_a/R.

mixture of a nonpolar solvent and a polar solvent, which is a good H-bond acceptor but a weak H-bond donor, its magnitude is given by:

$$K_a = \frac{K_1}{1 + K_S[\text{polar solvent}]} \quad (5)$$

where K_1 and K_S relate to the equilibria in eqs 3 and 4 above. The free energy change associated with the formation of the D•A association complex is determined by K_a:

$$\Delta G^\circ = -RT \ln K_a \quad (6)$$

Solution-phase experiments show that as the concentration of S2 is increased, log K_a remains constant at the value measured in pure S1, log K_1, until log[S2] approaches a value equal to −log K_S, after which it decreases as the concentration of the polar solvent is increased.[25] Figure 1 shows that solvation thermodynamics (black line) and the solvation state of D (green line) vary in a very different way as a function of solvent composition.

One of us has shown previously that solvation may be understood, at the molecular level, by considering the polarities and concentrations of the functional groups present in a liquid mixture.[25] The free energy of interaction may be calculated as the sum of the pairwise interactions between solute and solvent:

$$-RT \ln K_1 = \Delta G^\circ = -(\alpha - \alpha_{S1})(\beta - \beta_{S1}) + 6\text{kJ mol}^{-1} \quad (7)$$

$$-RT \ln K_S = \Delta G^\circ = -(\alpha - \alpha_{S1})(\beta_{S2} - \beta_{S1}) + 6\text{kJ mol}^{-1} \quad (8)$$

In eqs 7 and 8, α is the H-bond donor parameter for D, β is the H-bond acceptor parameter for A, α_{S1}, β_{S1} and β_{S2} are the corresponding solvent H-bond parameters,[27] and the constant of 6 kJ mol^{-1} is the free energy penalty for formation of a bimolecular complex between two solutes (approximately constant irrespective of the nature of the solvent). Values of the H-bond parameters have been tabulated and used to predict K_1 and K_S. Studies of H-bonding interactions in a wide range of media have corroborated this model, and values[25,26] enabling both K_1 and K_s to be calculated based on the polarities of the functional groups of the molecules in both the medium (solvent) and also the H-bonded complex (the solute).

For an AFM probe, the pull-off force is thought to be related to the interfacial tension at the probe-surface contact;[3,28] while this is expected to be influenced by the medium, the precise relationship between the work of adhesion and the association interactions between solvent molecules and the probe surface remains unclear.

Adhesion in Acetone/Heptane Mixtures. H-bond adhesive interactions were first characterized by AFM. Probes were coated with gold followed by a SAM of 11-hydroxyundecyl-1-thiol (HUT), yielding a hydroxyl-terminated tip. Adhesion (pull-off) forces (F_a) were measured between these probes and SAMs of HUT on gold or films of diethoxy(phosphatoethyl)triethoxysilane (DPTS) formed on glass. HUT is both an H-bond donor and acceptor, but DPTS is only an H-bond acceptor. Moreover, the packing density of DPTS is expected to be lower than that of HUT (although it is not known exactly). However, in the bulk phase, both interactions (i.e., HUT-HUT and HUT-DPTS) are governed by the equilibria associated with solvation of the hydroxyl-functionalized probe.

In pure heptane, pull-off forces of 5.12 and 1.95 nN were measured for hydroxyl functionalized probes interacting with HUT and DPTS films, respectively. As acetone was added to the liquid phase, the adhesion force remained constant initially, but at a certain point began to decrease and thereafter declined monotonically with log[acetone], reaching limiting values of

dx.doi.org/10.1021/la304246e | Langmuir 2012, 28, 17709−17717

0.33 nN and 0.23 nN in pure acetone for HUT and DPTS surfaces, respectively [Figure 1(b)].

Figure 1(a) indicates that K_S, the equilibrium constant for solvation of hydroxyl functionalized surfaces by acetone, can be determined from the concentration of acetone at which the flat section of the F_a−concentration plot intersects sloped portion. The intersection is at a concentration given by log[acetone] = $-K_S$. Values of 0.28 and 0.40 mol dm^{-3} were obtained from Figure 1(b) for HUT and DPTS surfaces, respectively, yielding a mean of 0.34 mol dm^{-3} (giving a K_S of 3 M^{-1} and an interaction free energy of −3 kJ mol^{-1} for the acetone-hydroxyl interaction). For solution-phase interactions, calculations using eq 8 yielded a value of K_S of 3 M^{-1} for solvation of hydroxyl groups by acetone in heptane (ΔG° = −3 kJ mol^{-1}), in exceptionally close agreement with the experimental value.

In contact mechanics, the adhesion force is usually related to the work of adhesion W ($F_a = 2\pi RW$ in the DMT model and $^3/_2\pi RW$ in the JKR). W depends upon the medium in which the interaction occurs. However, the relationship is a rather nonspecific one. In the present case, the acquisition of data in a liquid mixture enables a more precise interpretation to be given for the behavior. The close similarity between the values of K_S obtained in solution and from the data in Figure 1(b) indicates that this association occurs with a similar free energy for both the bulk phase molecules and for the case where the hydrogen bond donor is tethered to an AFM probe. By inference, these data also suggest that determination of K_S from a plot of F_a against solvent concentration may provide a general method for determining free energies of interaction at interfaces; by changing the composition of the liquid, the nature of the interfacial interactions should change and it should be possible to determine the corresponding K_S. An important corollary to this is that for any given liquid mixture, $F_a \alpha K_a$, and hence $F_a \alpha \Delta G$ where ΔG is the free energy change associated with the formation of a 1:1 association complex between the functional groups attached to the tip and surface.

Contact Mechanics in Acetone/Heptane Mixtures. The correlation between solution-phase thermodynamics and contact mechanics was examined. Figure 2 shows friction-load plots for HUT and DPTS surfaces in acetone:heptane mixtures, and also in two alcohols, ethanol and pentanol (a more complete set of data is given in the Supporting Information). In all three polar liquids, as well as in a 3:1 acetone:heptane mixture, HUT and DPTS both yielded a linear friction-load relationship, consistent with Amontons' law:

$$F_F = \mu F_N \quad (9)$$

where F_F is the friction force, F_N is the load applied perpendicular to the surface, and μ is the coefficient of friction. However, in a 1:1 acetone:heptane mixture, deviations from linearity were observed. For smaller acetone concentrations, and in pure heptane, the relationship was nonlinear (for both HUT and DPTS) and could be analyzed using the General Transition Equation of Carpick et al,[29] which yields a "transition parameter", α that indicates whether Johnson−Kendall−Roberts (JKR)[9] or Derjaguin−Muller−Toporpov (DMT)[10] mechanics fit the data. Fits to the experimental data using the General Transition Equation are shown in the Supporting Information. A transition parameter of ca. 0 was obtained for all, indicating that DMT mechanics applied.[10] Significantly, it was observed that linear friction-load relationships were only observed for liquid mixtures in which solution-phase measurements indicate that hydroxyl groups are

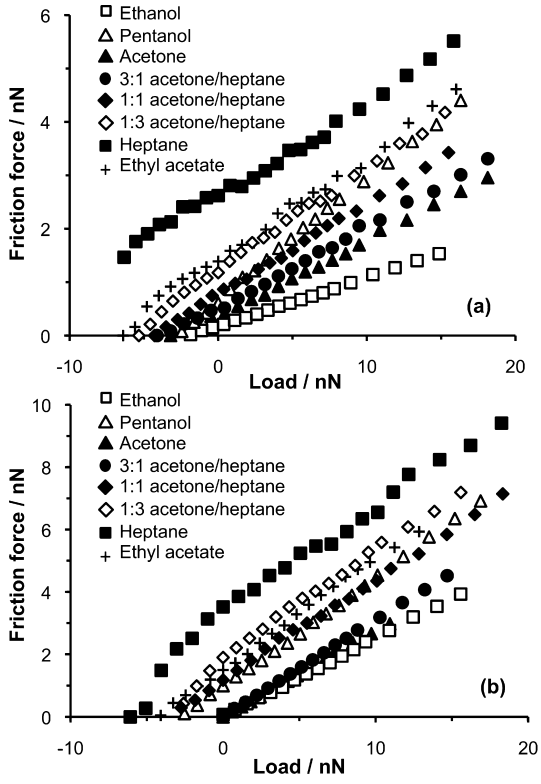

Figure 2. Friction-load plots for HUT-functionalized gold-coated probes interacting with (a) HUT and (b) DPTS surfaces in pure liquids and in acetone/heptane mixtures. For clarity, error bars have been omitted. However, a version of this figure that includes error bars is provided in the Supporting Information.

extensively solvated by the polar solvent, acetone (see Figure 1(a) for the relationship between the degree of solvation and the liquid composition).

These observations are in very good agreement with the data reported previously for interactions between carboxylic acid terminated SAMs.[17,19] In a recent paper by Gao et al., it was suggested that a linear friction-load relationship is "normal" for nanoscale molecular contacts, and there is no reason to expect the friction force to vary with the area of contact (as has been assumed for many years following the work of Tabor).[30] They suggested that nonlinear friction-load relationships are characteristic of limiting circumstances where adhesion is very strong. However, the data in Figure 2 are not consistent with such an explanation. The only mixtures in which linear friction-load relationships were observed were those for which solution-phase experiments predict extensive solvation of the H-bond donor, suggesting that a linear friction-load relationship represents a limiting type of behavior.

An alternative approach to understanding these observations is to treat the friction force as the sum of a load- or pressure-dependent term and an area-dependent shear term,[2,18] as in eq 1. This equation can be fit to the experimental data to yield two variable parameters, μ and $(\tau/K^{2/3})$. The value of μ is here described as the "coefficient of friction", although its meaning (see Discussion below) may be different from that which is usually associated with the coefficient of friction, and the value of $(\tau/K^{2/3})$ provides a relative or effective measure of the surface shear strength. It might be argued that the first term in eq 1 should be independent of the adhesion force and that F_a should not be included in it. However, fitting using such a

dx.doi.org/10.1021/la304246e | Langmuir 2012, 28, 17709−17717

modified form of the equation yielded the result that μ varied strongly with F_a, which plainly contradicts the initial premise (that F_a should not be included because μ is independent of F_a). Moreover, correcting the load to account for adhesion in the second term and not in the first is plainly inconsistent. Fits to the data using eq 1 are shown in the Supporting Information.

Figure 3 shows the values of μ and $(\tau/K^{2/3})$ as a function of the adhesion force, F_a, obtained by fitting using eq 1. Data are

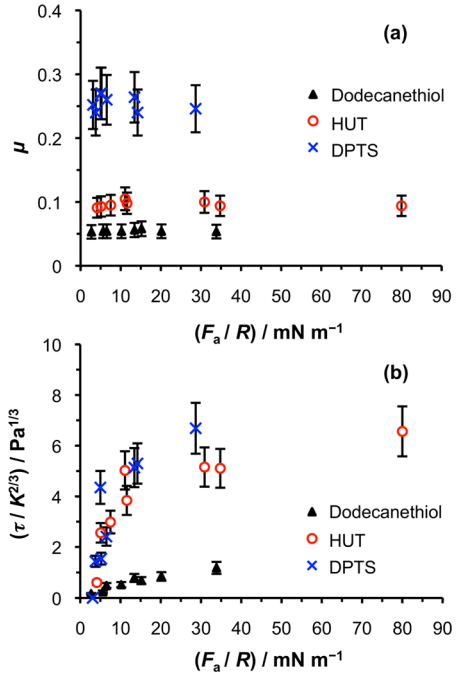

Figure 3. (a) Variation in the load-dependent "coefficient of friction" with the adhesion force for monolayers of dodecanethiol and HUT on gold, and films of DPTS on SiO_2. (b) Variation in the surface shear strength with the pull-off force.

also shown for a hydrophobic SAM, dodecanethiol on gold. For all three of the systems studied, μ was invariant with F_a. Dodecanethiol and HUT SAMs yielded similar values of μ, but a much larger value was obtained for DPTS. The alkylthiolate monolayers are expected to yield ordered, close-packed arrangements of alkyl chains, while silane films are known to be less close-packed and more disordered. Consequently, more pathways are available in DPTS films for energy dissipation, through deformation of the adsorbate conformation (for example, via the creation of gauche defects[31−33]) than is the case for the HUT and dodecanethiol films.

Classically speaking, friction has been regarded as being the sum of shear (adhesive) and plowing components.[8] The invariance of μ with F_a strongly suggests that it results from dissipative processes that do not involve adhesive interactions. We attribute these to a kind of molecular plowing mechanism, similar to that proposed by Carpick and co-workers.[34] Plowing is often associated with plastic deformation (in metallic systems, for example), but an alternative molecular plowing mechanism applicable to monolayers is defined by Brukman et al.,[35] in which "a portion of the energy expanded to deform the molecules mechanically is not recovered but is instead dissipated". In such a mechanism, dissipation may occur through molecular pathways that do not involve plastic deformation. The relative similarity in the values of μ for the two alkylthiolate SAMs, despite their very different surface free energies, is consistent with this explanation, reflecting their similar and rather close packing, and hence the similarity in the likely energy dissipation mechanisms.[36,37] The fact that there is nevertheless a difference in the coefficient of friction measured for the two alkylthiolate requires explanation and is addressed later.

SAMs of HUT yielded values of $(\tau/K^{2/3})$ five times larger than for the dodecanethiol SAM, but very similar to the value for DPTS, confirming that the shear strength in eq 5 is indeed strongly dependent on tip−sample adhesion. The striking closeness of the values of $(\tau/K^{2/3})$ for the two H-bonding systems in Figure 3(b) suggests that this parameter is strongly determined by the thermodynamics of the H-bonding interactions at the tip−sample contact: for liquids that solvate the surface extensively, small values of $(\tau/K^{2/3})$ were obtained, and these increased as the surface became less fully solvated, approaching a limiting value for the pure hydrocarbon solvent. The net adhesion force is smaller for DPTS because of the reduced density of H-bond acceptor sites at the surface, compared to an HUT SAM.

Figure 4 shows the surface shear strength $(\tau/K^{2/3})$ as a function of the concentration of acetone. The similarity

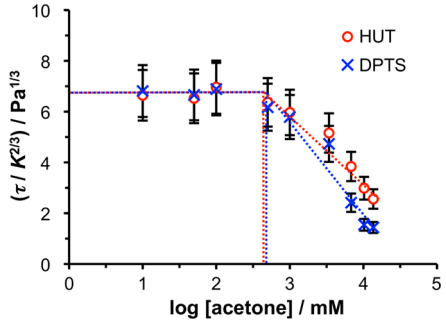

Figure 4. Variation in the surface shear strength, $(\tau/K^{2/3})$, with the composition of heptane:acetone mixtures.

between Figure 4 and the data in Figure 1 is striking. As the concentration of acetone increases, the magnitude of $(\tau/K^{2/3})$ at first remains constant, but then decreases, and exhibits a linear correlation with log[acetone]. The intersection between the horizontal and sloped portions of the graph occurs at ca. 2.7, for DPTS and HUT, compared with a value of 2.5 in Figure 1(b). Such remarkably close agreement suggests that for these molecular systems, $(\tau/K^{2/3})$ is proportional to the free energy of interaction at the tip−sample interface; measurements of the surface shear strength thus yield the equilibrium constant for solvation of hydroxyl functionalized surfaces by acetone, K_S. These observations are in accordance with the classical picture of area-dependent adhesive friction proposed by Bowden and Tabor.[8]

Contact Mechanics for Mixed Surfaces. To explore further the correlation between thermodynamics and contact mechanics, measurements were made for mixed SAMs formed by partial photo-oxidation of HUT SAMs. An unresolved question concerns whether the transition to a linear friction-load relationship is determined only by the net strength of adhesion, or whether the thermodynamics of the H-bond donor/solvent interaction are dominant. In an earlier study for carboxylic acid terminated SAMs, Busuttil et al. found that for mixed $COOH/CH_3$ SAMs interacting with COOH-function-

dx.doi.org/10.1021/la304246e | Langmuir 2012, 28, 17709−17717

alized probes in heptane, nonlinear friction-load relationships were acquired even at low concentrations of COOH in the surface, when the adhesion force was small. It was concluded that the thermodynamics of the tip-solvent interaction is more important than the magnitude of the adhesion force in determining the contact mechanics. Here we extend the approach to hydroxyl-functionalized probes, and also model the contact mechanics to examine the relationship between the interfacial thermodynamics and the coefficient of friction and surface shear strength.

Mixed OH/CH_3 SAMs were formed by exposing HUT SAMs to UV light for varying periods of time, causing partial photo-oxidation of adsorbates. The samples were immersed in a solution of dodecanethiol (DDT), causing displacement of the oxidized HUT molecules and an increase in the advancing water contact angle [Figure 5(a)]. As the exposure increased,

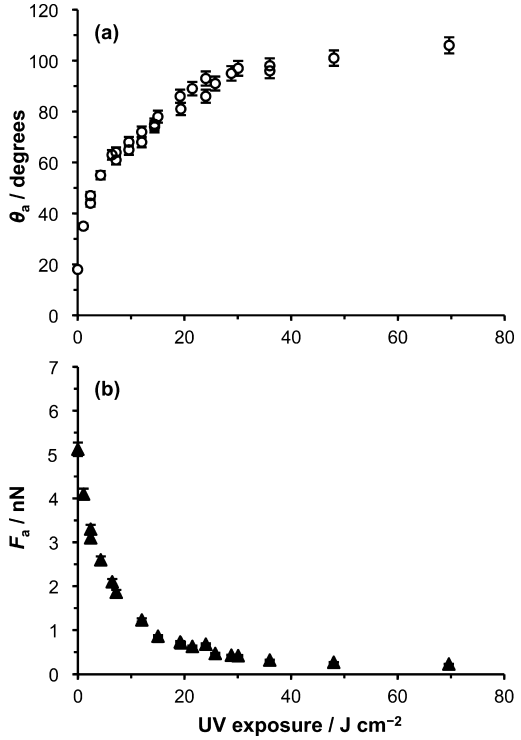

Figure 5. Variation in the advancing water contact angle (a) and pull-off force in heptane (b) with UV exposure for HUT SAMs following postexposure immersion in a solution of dodecanethiol in ethanol.

the contact angle approached a limiting value of 106°, similar to that of a dodecanethiol monolayer. After an exposure of ca. 30 J cm^{-2}, the contact angle had increased close to the limiting value, and thereafter it changed slowly. As the contact angle increased, the pull-off force decreased [Figure 5(b)], as the contribution of H-bonding to the tip−sample adhesive interaction decreased. For a complete HUT SAM, a pull-off force of 5.1 nN was measured; as the exposure was increased and more of the HUT replaced by DDT, F_a decreased to 0.4 nN after 30 J cm^{-2} and approached a limiting value of ca. 0.2 nN.

Samples were characterized by X-ray photoelectron spectroscopy (XPS). C1s spectra were acquired at high resolution (see Supporting Information). Two components were fitted to the spectrum for virgin HUT, at 285.0 eV corresponding to the alkyl chain and at 286.7 eV corresponding to the carbon atom adjacent to the hydroxyl group, designated C−O. The ratio of the area of the C−O component to the area of the whole C1s peak was used to quantify the composition of the samples. For HUT, attenuation of the signal from the alkyl chain meant that the area of the C−O component was larger than indicated by the stoichiometry of the adsorbate, and the [C−O]/[C1s] ratio was thus 0.127. As exposure increased, the [C−O]/[C1s] ratio decreased, approaching 0 in the limit of complete replacement of HUT by DDT. The contact angle data were transformed to cos θ, which is proportional to the surface free energy[38] and should be proportional to the fraction of polar terminal groups at the surface. The variation in cos θ and F_a with the [C−O]/[C1s] ratio is shown in Figure 6. It can be seen that, as

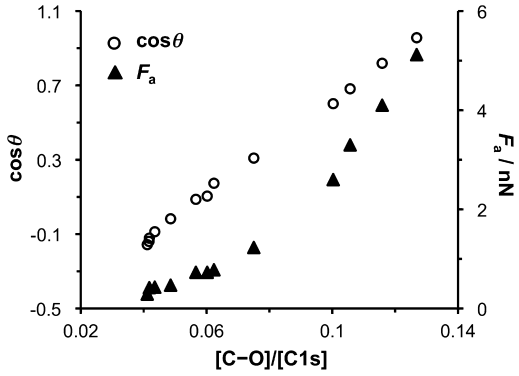

Figure 6. Variation in cos θ and F_a with the composition of HUT samples exposed to UV light for varying periods of time and immersed in a solution of DDT.

expected, the relationship between cos θ and the [C−O]/[C1s] ratio is linear. F_a also varies with the composition, but in a different way. At high [C−O]/[C1s] values, F_a decreases steeply with decreasing values of [C−O]/[C1s]. However, between [C−O]/[C1s] values of 0.1 and 0.075, there is a change in slope and F_a decreases less rapidly.

Friction-load plots were acquired as a function of the UV exposure (Figure 7). For exposures as large as 30 J cm^{-2}, which gave rise to extensive surface modification, the friction-load plot was found to be nonlinear. Only at the largest exposure studied, 70 J cm^{-2}, did the friction-load plot approximate to linearity. For all other exposures, the friction-load plots were nonlinear. The data were fitted using eq 1, and for each system, the values of μ and $(\tau/K^{2/3})$ were obtained. These values are shown in

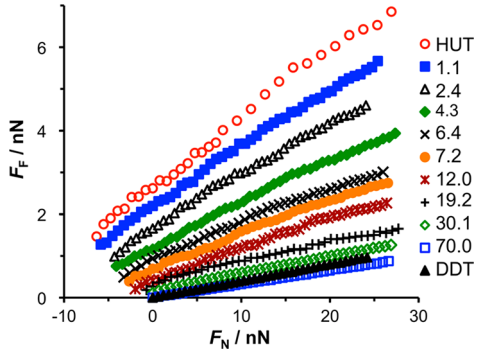

Figure 7. Friction-load plots for HUT-functionalized gold-coated probes interacting with HUT SAMs that have been subjected to varying UV exposures and immersed in a solution of DDT in ethanol. The numbers in the legend give exposure/J cm^{-2}.

dx.doi.org/10.1021/la304246e | *Langmuir* 2012, 28, 17709−17717

Figure 8 as a function of the composition of the samples determined by XPS, to facilitate comparison with Figure 6.

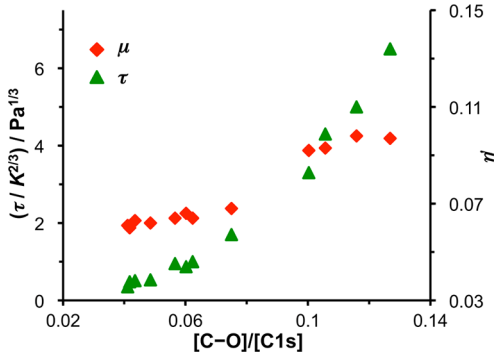

Figure 8. Variation in $(\tau/K^{2/3})$ and μ with the composition of HUT samples exposed to UV light for varying periods of time and immersed in a solution of DDT.

It is clear that the value of $(\tau/K^{2/3})$ varies markedly with the composition of the film, increasing by over an order of magnitude from the most heavily modified samples to the virgin HUT. The variation in $(\tau/K^{2/3})$ with composition correlates extremely closely with the variation in F_a with composition, supporting the hypothesis that the surface shear strength is dominated, in these materials, by the adhesive forces that result from H-bonding between the tip and the surface. However, the variation in μ with composition is rather different. For $[C{-}O]/[C1s] \geq 0.1$, very similar values of μ are obtained for all materials, and these values are all close to the mean value of μ for the HUT/HUT couple in Figure 3(a) (0.096). For $[C{-}O]/[C1s] \leq 0.75$, very similar values of μ are obtained also for all materials, but for these samples, the values are all close to the mean value of μ for the HUT/DDT couple in Figure 3(a) (0.055).

It was noted above, in relation to Figure 3(a), that the values of μ for the alkylthiolates were similar, and rather different from the value measured for DPTS films, and this was interpreted in terms of the different packing densities of the two materials. Nevertheless, the ratio of μ_{HUT}:μ_{DDT} was ca. 2:1, so the values were certainly not identical. The data in Figure 8 point to a possible explanation. There is an abundance of literature that demonstrates that the coefficients of friction of alkylthiolate SAMs vary with the nature of the terminal functional group.[6,13,18,39−46] In particular, hydroxyl and carboxylic acid terminated SAMs yield coefficients of friction that are significantly larger than those of methyl terminated SAMs. If μ reflects energy dissipation in molecular plowing, as we have hypothesized above, why does μ appear to depend on the nature of the terminal group? The data in Figure 8 show that while μ is different for $[C{-}O]/[C1s] \leq 0.75$ and for $[C{-}O]/[C1s] \geq 0.1$, there is not, apparently, a simple correlation with the composition in the way that variations in $(\tau/K^{2/3})$ are correlated with changes in the composition. We suggest that the change in μ results not from a change in adhesion, but from a change in the molecular plowing resulting from altered intermolecular interactions. A characteristic of hydroxyl and carboxylic acid groups is that they may form intramonolayer H-bonded networks. It has already been suggested that such H-bonded networks may influence the frictional properties of these SAMs.[6,46] We suggest that the samples that yield the largest values of μ in Figure 8 are those that have large enough HUT concentrations to enable the formation of H-bonded intramonolayer networks. At a critical composition, for $1.0 > [C{-}O]/[C1s] > 0.75$, the density of HUT becomes sufficiently low that such an H-bonded network does not form. Consequently, much less work has to be done during plowing to disrupt lateral H-bond interactions, and the coefficient of friction drops abruptly.

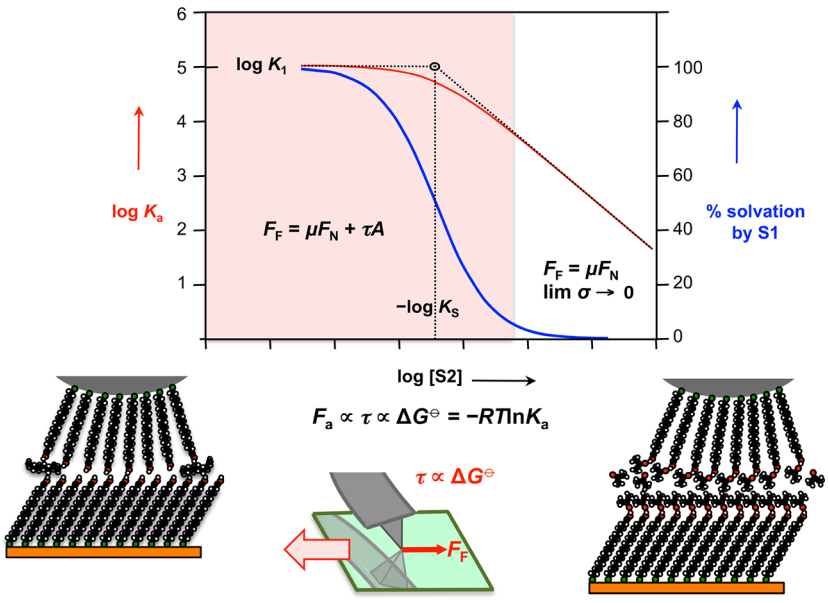

Figure 9. A "phase diagram" showing (red curve) the variation in log K_a for the formation of a 1:1 H-bonded association complex with the composition of the liquid medium for mixtures of acetone (S2) and heptane (S1); (blue curve) the associated variation in the % solvation of the H-bond donor by acetone; and the accompanying "phases" in which the contact mechanics exhibit either sublinear (pink shading) or linear (unshaded) dependence on the load. A linear friction-load relationship is associated with a very high degree of solvation and represents the limiting case that the surface shear strength tends to zero.

dx.doi.org/10.1021/la304246e | *Langmuir* 2012, 28, 17709−17717

While lateral H-bonding interactions cannot explain all of the correlations that have been reported between SAM terminal group chemistry and friction, it seems likely that many similar explanations (in terms of molecular plowing phenomena) may exist.

Summary. Figure 9 provides a global overview of the regimes delineated here. At low concentrations of the polar (hydrogen-bond-accepting) solvent, log K_a is equal to log K_1, the value measured in pure hydrocarbon, and varies little with concentration. Under these conditions, a sublinear friction-load relationship is observed. When log[polar solvent] equals −log K_S, the value of log K_a begins to fall. As it does so, the adhesion force and the surface shear strength, both of which are proportional to log K_a, also fall. When the degree of solvation approaches 100%, a limit of weak adhesion is reached. The area-dependent term in eq 1 becomes small compared to the load-dependent term. The adhesive interaction between the probe is dominated by dispersion interactions, and an approximately linear friction-load relationship is observed.

These findings suggest an approach to constructing a unified framework for interpreting nanoscale tribological measurements. They also indicate that nanoscale tribological data may provide a powerful tool for the prediction of thermodynamic quantities associated surface equilibria, enabling thermodynamic properties to be predicted quantitatively for interfacial interactions. The relationship between the contact mechanics and solution-phase thermodynamic quantities may, moreover, provide a theoretical framework for the design of customized surfaces with specific adhesion and friction properties.

CONCLUSIONS

The literature reveals a broad range of different approaches to the quantitative analysis of friction force microscopy data from molecular systems. The results presented here suggest that the apparent contradictions inherent in previously published works may dissolve when the friction force is treated, as others have suggested, as the sum of load-dependent and area-dependent terms. For organic monolayers that form interfacial hydrogen bonds, we attribute the load-dependent term to molecular plowing, in which energy is dissipated in the conformational deformation of molecules in the contact area. The coefficient of friction is independent of the strength of tip−sample adhesion. The area-dependent shear term is characterized by a surface shear strength that is proportional to the bulk, solution-phase free energy of interaction of the terminal groups interacting across the tip−sample contact; it is closely correlated with the pull-off force. Importantly, the variation of the surface shear strength with the properties of the liquid medium correlates closely with, and may be used to predict, bulk thermodynamics quantities (equilibrium constants) associated with the monolayer-solvent interaction. In the limit of complete solvation of the hydrogen bond donors at the interface by polar molecules from the liquid medium, the shear term approaches zero, and a linear friction-load relationship results. For partially solvated surfaces, and in hydrocarbon media, the friction-load plot is fitted by DMT mechanics.

ASSOCIATED CONTENT

Supporting Information

An alternate version of Figure 2 that includes error bars; fits to the friction-load data using the General Transition Equation and using eq 1; C1s spectra of mixed SAMs formed by photooxidation and replacement of oxidized adsorbates. This material is available free of charge via the Internet at http://pubs.acs.org."

AUTHOR INFORMATION

Corresponding Author

*E-mail: Graham.Leggett@sheffield.ac.uk.

Notes

The authors declare no competing financial interest.

ACKNOWLEDGMENTS

The authors thank EPSRC (Grant EP/039999/1) for financial support.

ABBREVIATIONS

HUT, 11-hydroxyundecyl-1-thiol; DPTS, diethoxy-phosphatoethyl-triethoxysilane

REFERENCES

(1) Overney, R.; Meyer, E. *MRS Bull.* **1993**, 26−34.
(2) Carpick, R. W.; Salmeron, M. *Chem. Rev.* **1997**, *97*, 1163−1194.
(3) Mate, C. M. *Tribology on the Small Scale*; Oxford University Press: Oxford, 2008.
(4) Frisbie, C. D.; Rozsnyai, L. F.; Noy, A.; Wrighton, M. S.; Lieber, C. M. *Science* **1995**, *265*, 2071−2074.
(5) McDermott, M. T.; Green, J.-B. D.; Porter, M. D. *Langmuir* **1997**, *13*, 2504−2510.
(6) Kim, H. I.; Houston, J. E. *J. Am. Chem. Soc.* **2000**, *122*, 12045−12046.
(7) Brewer, N. J.; Beake, B. D.; Leggett, G. J. *Langmuir* **2001**, *16*, 735−739.
(8) Bowden, F. P.; Tabor, D. *The Friction and Lubriction of Solids*; Oxford University Press: Oxford, 1950.
(9) Johnson, K. L.; Kendall, K.; Roberts, A. D. *Proc. R. Soc. London A* **1971**, *324*, 301−313.
(10) Derjaguin, B. V.; Muller, V. M.; Toporov, Y. P. *J. Colloid Interface Sci.* **1975**, *53*, 314−325.
(11) Muller, V. M.; Derjaguin, B. V.; Toporov, Y. P. *Colloids Surf.* **1983**, *7*, 251−259.
(12) Clear, S. C.; Nealey, P. F. *J. Colloid Interface Sci.* **1999**, *213*, 238−250.
(13) Clear, S. C.; Nealey, P. F. *Langmuir* **2001**, *17*, 720−732.
(14) Ruths, M. *J. Phys. Chem. B* **2006**, *110*, 2209−2218.
(15) Hurley, C. R.; Leggett, G. J. *Langmuir* **2006**, *22*, 4179−4183.
(16) Colburn, T. J.; Leggett, G. J. *Langmuir* **2007**, *23*, 4959−4964.
(17) Busuttil, K.; Geoghegan, M.; Hunter, C. A.; Leggett, G. J. *J. Am. Chem. Soc.* **2011**, *133*, 8625−8632.
(18) Marti, A.; Hähner, G.; Spencer, N. D. *Langmuir* **1995**, *11*, 4632−4635.
(19) Busuttil, K.; Nikogeorgos, N.; Zhang, Z.; Geoghegan, M.; Hunter, C. A.; Leggett, G. J. *Faraday Discuss.* **2012**, *156*, 325−341.
(20) Hutter, J. L.; Bechhoefer, J. *Rev. Sci. Instrum.* **1993**, *64*, 1868−1873.
(21) Ogletree, D. F.; Carpick, R. W.; Salmeron, M. *Rev. Sci. Instrum.* **1996**, *67*, 3298−3306.
(22) Varenberg, M.; Etsion, I.; Halperin, G. *Rev. Sci. Instrum.* **2003**, *74*, 3362−3367.
(23) Zenhausen, F.; Adrian, M.; Heggeler-Bordied, B. T.; Eng, L. M.; Descouts, P. *Scanning* **1992**, *14*, 212−217.
(24) .
(25) Buurma, N. J.; Cook, J. L.; Hunter, C. A.; Low, C. M. R.; Vinter, J. G. *Chem. Sci.* **2010**, 242−246.
(26) Cook, J. L.; Hunter, C. A.; Low, C. M. R.; Perez-Velasco, A.; Vinter, J. G. *Angew. Chem., Int. Ed.* **2007**, *46*, 3706−3709.
(27) Hunter, C. A. *Angew. Chem., Int. Ed.* **2004**, *43*, 5310−5324.
(28) Israelachvilli, J. N. *Intermolecular and Surface Forces*, 2nd ed.; Academic Press: London, 1992.

(29) Carpick, R. W.; Ogletree, D. F.; Salmeron, M. *J. Colloid Interface Sci.* **1999**, *211*, 395−400.
(30) Gao, J.; Luedtke, W. D.; Gourdon, D.; Ruths, M.; Israelachvili, J. N.; Landman, U. *J. Phys. Chem. B* **2004**, *108*, 3410−3425.
(31) Tutein, A. B.; Stuart, S. J.; Harrison, J. A. *Langmuir* **1999**, *16*, 291−296.
(32) Mikulski, P. T.; Harrison, J. A. *J. Am. Chem. Soc.* **2001**, *123*, 6873−6881.
(33) Mikulski, P. T.; Herman, L. A.; Harrison, J. A. *Langmuir* **2005**, *21*, 12197−12206.
(34) Flater, E. E.; Ashurst, W. R.; Carpick, R. W. *Langmuir* **2007**, *23*, 9242−9252.
(35) Brukman, M. J.; Marco, G. O.; Dunbar, T. D.; Boardman, L. D.; Carpick, R. W. *Langmuir* **2006**, *22*, 3988−3998.
(36) Tutein, A. B.; Stuart, S. J.; Harrison, J. A. *J. Phys. Chem. B* **1999**, *103*, 11357−11365.
(37) Mikulski, P. T.; Gao, G.; Chateauneuf, G. M.; Harrison, J. A. *J. Chem. Phys.* **2005**, *122*, 024701.
(38) Adamson, A. W.; Gast, A. P. *Physical Chemistry of Surfaces*, 6th ed.; Wiley, 1997.
(39) Frisbie, C. D.; Rozsnyai, L. F.; Noy, A.; Wrighton, M. S.; Lieber, C. M. *Science* **1994**, *265*, 2071−2074.
(40) Kim, H. I.; Koini, T.; Lee, T. R.; Perry, S. S. *Langmuir* **1997**, *13*, 7192−7196.
(41) van der Vegte, E. W.; Hadziioannou, G. *Langmuir* **1997**, *13*, 4357−4368.
(42) Beake, B. D.; Leggett, G. J. *Phys. Chem. Chem. Phys.* **1999**, *1*, 3345−3350.
(43) Kiely, J. D.; Houston, J. E. *Langmuir* **1999**, *15*, 4513−4519.
(44) Kim, H. I.; Graupe, M.; Oloba, O.; Koini, T.; Imaduddin, S.; Lee, T. R.; Perry, S. S. *Langmuir* **1999**, *15*, 3179−3185.
(45) Beake, B. D.; Leggett, G. J. *Langmuir* **2000**, *16*, 735−739.
(46) Brewer, N. J.; Beake, B. D.; Leggett, G. J. *Langmuir* **2001**, *17*, 1970−1974.